Applied Catalysis B: Environmental 181 (2016) 874–887

Contents lists available at ScienceDirect

Applied Catalysis B: Environmental

journal homepage: www.elsevier.com/locate/apcatb

A combined experimental and computational study of the mechanism of fructose dehydration to 5-hydroxymethylfurfural in dimethylsulfoxide using Amberlyst 70, PO_4^{3-}/niobic acid, or sulfuric acid catalysts

Jing Zhang[a], Anirban Das[a], Rajeev S. Assary[b], Larry A. Curtiss[b,**], Eric Weitz[a,*]

[a] Department of Chemistry and Institute for Atom Efficient Chemical Transformations, Northwestern University, Evanston, IL 60208, USA
[b] Institute for Atom Efficient Chemical Transformations, Materials Science and Chemistry Divisions, Argonne National Laboratory Argonne, IL 60439, USA

ARTICLE INFO

Article history:
Received 17 July 2014
Received in revised form 17 October 2014
Accepted 21 October 2014
Available online 1 November 2014

Keywords:
Fructose dehydration
Mechanism
NMR spectroscopy
Isotope labeling studies
G4MP2 calculations

ABSTRACT

We report on a combined experimental and theoretical study of the acid catalyzed dehydration of D-fructose in dimethylsulfoxide (DMSO) using; Amberlyst 70, PO_4^{3-}/niobic acid, and sulfuric acid as catalysts. The reaction has been studied and intermediates characterized using; ^{13}C, ^{1}H, and ^{17}O NMR, and high resolution electrospray ionization mass spectrometry (HR ESI–MS). High level G4MP2 theory calculations are used to understand the thermodynamic landscape for the reaction mechanism in DMSO. We have experimentally identified two key intermediates in the dehydration of fructose to form HMF that were also identified, using theory, as local minima on the potential surface for reaction. A third intermediate, a species capable of undergoing keto–enol tautomerism, was also experimentally detected. However, it was not possible to experimentally distinguish between the keto and the enol forms. These data with different catalysts are consistent with common intermediates along the reaction pathway from fructose to HMF in DMSO. The role of oxygen in producing acidic species in reactions carried out in DMSO in presence of air is also discussed.

1. Introduction

Naturally occurring, abundant and accessible carbohydrates are viewed as promising and underexploited "green" and renewable resources which can be used to produce chemical feedstocks and liquid transportation fuels [1]. Sugars, including both D-fructose and glucose, are a class of carbohydrates that can be used to produce chemical feedstocks[2,3]. 5-Hydroxymethylfurfural (HMF), has generated considerable scientific interest as a versatile biomass-derived chemical feedstock from which compounds can be generated that can then be utilized in a wide variety of chemical applications [4–6]. Rosatella et al. [4] describe a biorefinery approach that would decrease dependence on fossil fuels. HMF is discussed as a useful intermediate in such an approach, as it could be converted into biofuels like dimethylfuran and chemical feedstocks such as furan dicarboxylic acid, gamma-valerolactone (GVL) and levulinic acid [7]. GVL could then be converted to methyltetrahydrofuran, a diesel additive, or it could act as a platform for the synthesis of adipic acid. Thus, Nylon could potentially be produced from chemicals synthesized from biomass. One convenient pathway to HMF is via the triple dehydration of fructose [8–10]. Isotope-labeling studies suggest that HMF production via the consecutive loss of three water molecules takes place preferentially from the cyclic furanose tautomer [11]. It has been shown that a wide variety of Lewis and Brønsted acids catalyze this reaction. These include mineral acids (HCl, H_2SO_4, and H_3PO_4) [12–14], transition metal ions [15–17], H-type zeolites [18], supported heteropolyacids [19], strongly acid cation-exchange resins [20,21], and solid metal phosphates [22–25]. This reaction has been studied in a variety of solvents including water, organic solvents, ionic liquids, organic/water mixtures, biphasic water/organic systems, and supercritical water [16,22–24,26–34]. Both the choice of catalyst and solvent can affect yields and the specificity for HMF formation. Some studies [33] have been carried out in DMSO in the presence of air. However, literature reports [35] indicate that at moderately high temperatures (~80 °C) DMSO decomposes into acidic

* Corresponding author at: Northwestern University, Chemistry, Evanston, IL 60208, USA. Tel.: +1 847 869 6155.
** Corresponding author at: Institute for Atom Efficient Chemical Transformations, Materials Science and Chemistry Divisions, Argonne National Laboratory, Argonne, IL 60208, USA. Tel : +1 630 252 7380.
E-mail addresses: curtiss@anl.gov (L.A. Curtiss), weitz@northwestern.edu (E. Weitz).

http://dx.doi.org/10.1016/j.apcatb.2014.10.056
0926-3373/

species, including sulfuric acid. We provide data that indicates that these species can catalyze the reaction in DMSO. In general, the yields of HMF are lower than desired because the dehydration reactions that lead to HMF are in competition with undesirable reactions, including reversion, fragmentation and polymerization [20]. Though there have been studies that focused on the mechanism of formation of HMF [34], it is still not clear how the choice of solvent and catalyst affects the production of HMF in preference to undesirable products. In addition, questions still remain about the identity of the intermediates in this process, the effect of solvent on their energies, and thus the commonality of these intermediates for different catalysts and solvents. As such, further investigation of these issues is desirable in order to establish a detailed molecular level mechanism for the reaction of fructose to HMF. Such a determination, for a number of different catalysts and solvents, has the potential to provide insights that could lead to the development of new catalysts tailored for improved yields and selectivity for HMF formation.

Haworth and Jones [36] suggested that the high selectivity of HMF formation from fructo-furanose is due to the structural similarity of the five-membered ring in both fructose and HMF; an extension of the observation that the fructofuranose ring system is more readily converted to 5-hydroxymethylfurfural than the glucopyranose system [11]. In prior studies, van Dam et al. [37], Kuster [38] and Antal et al. [39] proposed mechanisms involving either acyclic or cyclic intermediates. Recently, based on ^{1}H and ^{13}C NMR data, Amarasekara et al. [33] identified a key cyclic intermediate as (4R,5R)-4-hydroxy-5-hydroxymethyl-4,5-dihydrofuran-2-carbaldehyde for fructose dehydration to form HMF in DMSO at 150 °C. A recent report by Kimura et al. [34] identified the intermediates 3,4-dihydroxy-2-dihydroxymethyl-5-hydroxymethyltetrahydrofuran and 4-hydroxy-5-hydroxymethyl-4,5-dihydrofuran-2-carbaldehyde by means of in-situ ^{13}C NMR spectroscopy. The latter is the same intermediate proposed by Amarasekara, while the former was previously unreported. Horvath et al. [40] proposed reaction pathways for the acid (H_2SO_4) catalyzed conversion of fructose to HMF involving the intermediates, (2R,3S,4S)-2-(hydroxymethyl)-5-(hydroxyl-methylene)tetrahydrofuran-3,4-diol and (4S,5R)-4-hydroxy-5-hydroxymethyl-4,5-dihydrofuran-2-carbaldehyde. The later is the same intermediate proposed by Kimura and Amarasekara except with a different chirality. Our previous study of this reaction [41] shows that the sequential dehydration of fructose to form HMF follows a similar mechanism in different solvents (DMSO and H_2O) and with different catalysts (PO_4^{3-}/niobic acid, Amberlyst 70, and H_2SO_4).

In this study, we report on the acid catalyzed dehydration of D-fructose in DMSO-d_6. The reaction intermediates and products were probed using ^{13}C, ^{1}H, and ^{17}O NMR spectroscopy. With the aid of ^{13}C NMR, ^{13}C-labeled fructose and high resolution electrospray ionization mass spectrometry (HR ESI–MS) we have identified two key intermediates in the reaction of fructose to form HMF in DMSO-d_6. A third species, capable of undergoing keto–enol tautomerism, was also experimentally identified, though it was not possible to uniquely identify which tautomer was present. This experimental work is coupled with a theoretical study of the free energies of various intermediates resulting in a proposed mechanism for this reaction in DMSO. The two intermediates whose structures were unambigiously identified experimentally are also identified by theory as minima on the potential energy surface for the dehydration of fructose in DMSO. Both the keto and enol forms of the third species are also local minima on the free energy surface with the keto form being lowest in energy.

This reaction was studied experimentally using three acid catalysts: Amberlyst 70, PO_4^{3-}/niobic acid or sulfuric acid in DMSO. Sulfuric acid is a homogeneous Brønsted acid. PO_4^{3-}/niobic acid and Amberlyst 70 are heterogeneous solid state catalysts. Niobic acid has both Lewis and Brønsted acidic sites [42] while Amberlyst 70 is a Brønsted acid. We note that typically in the reactions previously reported in the literature that are alluded to above that used DMSO as a solvent, no effort was made to exclude air. Maintaining consistency with previous literature reports, this report presents data collected in the presence of air; however data collected in an inert atmosphere are also presented to demonstrate the effect of oxygen on reactions carried out at moderate temperatures in DMSO.

The three intermediates which we have experimentally identified in this work are shown in Scheme 1. **Int. 3**, 4-(hydroxy)-5-(hydroxymethyl)-4,5-dihydrofuran-2-carbaldehyde, was previously reported by Horvath [40], Amarasekara [33] and Kimura, though with different conclusions with regard to chirality [34]. We have not investigated its chirality. Another species (**Int. 2**) may exist either as an enol form, 2-(hydroxymethyl)-5-(hydroxylmethylene)-tetrahydrofuran-3,4-diol or a keto form 3,4-dihydroxy-5-hydroxymethyl-tetrahydro-furan-2-carbaldehyde. The enol form was reported by Horvath, but was postulated as a solvated transition state by Amarasekara. **Int. 1** in Scheme 1 is a DMSO complex with 2,6-anhydro-β-D-fructofuranose which we name as 2-(hydroxydimethylsulfinyloxy)-β-D-fructofuranose that has not been previously reported.

2. Experimental section

2.1. Materials

(−)-D-Fructose (>99.9%), DMSO-d_6 (99.9% atom D), D_2O (99.9% atom D), $H_2{}^{17}O$ (22.0 at%), phosphoric acid (85 wt%), 5-hydroxymethylfurfural (HMF) (≥99%), sulfuric acid (H_2SO_4, 98 wt%), and biphenyl (99.5%) were obtained from Sigma-Aldrich and used without further purification. Amberlyst 70 (a sulfonic ion-exchange resin) was purchased from Sigma-Aldrich as wet beads and was dried overnight in an oven at 60 °C [^{13}C-1]. Fructose, [^{13}C-2] fructose, and [^{13}C-6] fructose (99 at%) were purchased from Omicron Biochemicals Inc. (IN). Niobic acid ($Nb_2O_5{\cdot}nH_2O$, containing 20 wt% H_2O) was kindly supplied by CBMM (Companhia Brasileira de Metalurgiae Mineracão). Preparation of the PO_4^{3-}/niobic acid catalyst followed procedures similar to those employed by Carlini et al. [23] in which 19.056 g of niobic acid was stirred in 360 ml of 1 M phosphoric acid (in DI H_2O) for 48 h. The suspension was centrifuged at 8500 rpm and the top water phase was decanted off. The solid obtained was washed three times with water using repeated centrifugation and decantation. The resulting washed solid was dried in a vacuum oven at 160 °C and then calcinated at 300 °C for 3 h to obtain the catalyst.

2.2. Nuclear magnetic resonance (NMR)

Fourier transform ^{13}C and ^{1}H NMR spectra were acquired on a Bruker Avance III 500 (DCH CryoProbe). NMR spectra were obtained at a base frequency of 125.71 MHz for ^{13}C and 499.95 MHz for ^{1}H. For ^{13}C NMR spectroscopy, the pulse sequence used a delay (D1) and acquisition times (AQ) of 2.0 and 1.0 s, respectively, a spectral width of 29.7 kHz, 32 K data points, 90° pulse (12.0 μs) and 256 scans. A ^{13}C NMR DEPT spectrum was obtained at $\theta z = 135°$ where CH and CH_3 signals appear in the positive phase and CH_2 appears in the negative phase. For the ^{1}H NMR experiment, D1 = 1.0 s, AQ = 3.2 s, a spectral width of 10.3 kHz, 64 K data points, 90° pulse (10.7 μs) and 16 scans were used. Chemical shifts are reported in ppm relative to DMSO-d_6 at 2.50 and 39.51 ppm for ^{1}H and ^{13}C NMR

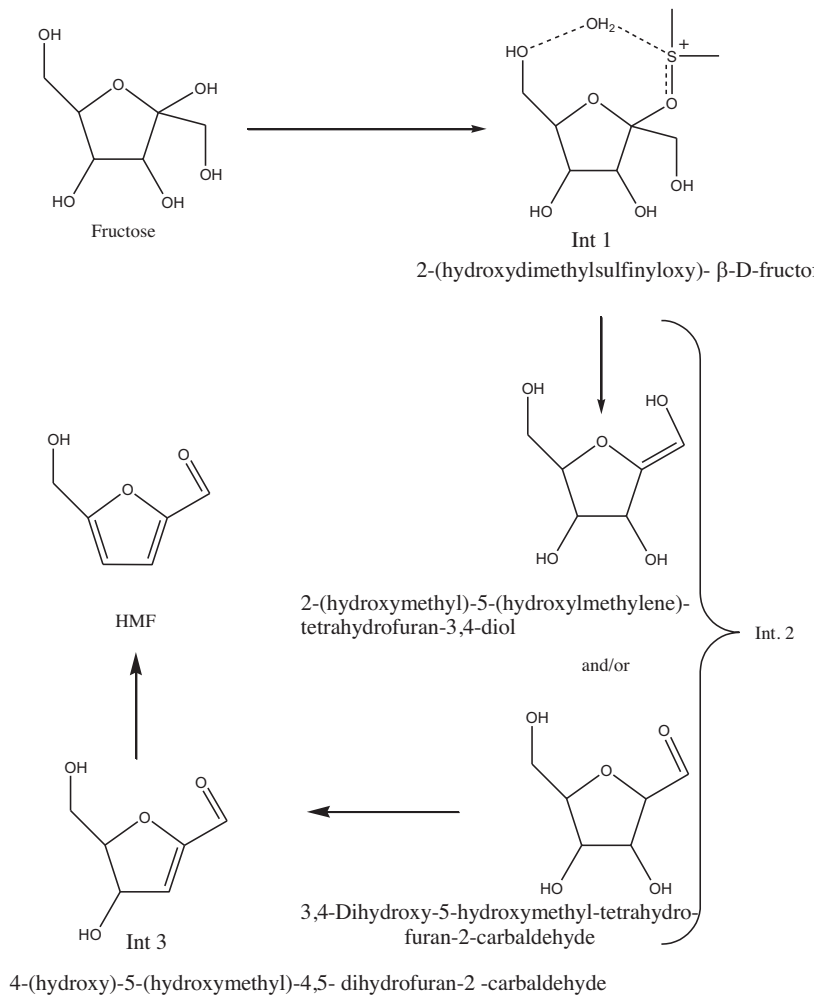

Scheme 1. Structure of HMF, the product of the acid catalyzed triple dehydration of fructose, and the previously reported intermediates formed during this reaction in DMSO.

spectra, respectively. In situ ^{17}O NMR spectra were acquired with 4092 scans on a Varian Inova-400 spectrometer.

2.3. Procedures for NMR studies on fructose dehydration in DMSO-d_6

Batch catalytic experiments for the dehydration of ~3 wt% fructose (0.904 g) in DMSO-d_6 (30 ml) were carried out in a 50 ml glass flask equipped with a magnetic stirrer and a reflux condenser. Biphenyl (0.3 g) was added as an internal standard. 0.075 g of Amberlyst 70 catalyst (the substrate/catalyst weight ratio was 12) was added to the reaction mixture which was then heated to the desired temperature (80–100 °C) by means of a temperature regulated oil bath. Aliquots of approximately 0.5 ml volume were periodically transferred to an NMR tube via a syringe for up to 48 h of reaction time. The reaction was quenched by immersing the NMR tube containing the sample in an ice-water bath. Prior to recording a ^{1}H or ^{13}C NMR spectrum the samples were thawed. Similar procedures were followed for fructose dehydration in DMSO-d_6 with the PO_4^{3-}/niobic acid catalyst where the substrate/catalyst weight ratio was also 12. Typically, 0.9 g of fructose, 0.3 g biphenyl and 0.075 g PO_4^{3-}/niobic acid were added to 30 ml DMSO-d_6 and the reaction mixture was heated at the desired temperature. For sulfuric acid catalyzed reactions, 1% v/v of 0.8 mM H_2SO_4 solution in DMSO was added. Standard Schlenk techniques were employed for reactions carried out under air-free conditions. The DMSO was dried using activated 3 Å molecular sieves under an inert atmosphere and injected into an evacuated Schlenk flask containing fructose and biphenyl and either Amberlyst 70 or PO_4^{3-}/niobic acid, which was back-filled with nitrogen. For the dehydration of ^{13}C-labeled fructose in DMSO-d_6, a solution of D-fructose (15 mg) in 0.5 ml of DMSO-d_6 and 1.3 mg PO_4^{3-}/niobic acid, sulfuric acid (10 mol%) or 1.3 mg Amberlyst 70 was prepared in a 5-mm J-Young NMR tube and transferred to the NMR spectrometer. ^{1}H and ^{13}C NMR spectra were recorded at room temperature. The NMR tube was then placed in a temperature regulated oil bath at 80 °C for a predetermined time, and the reaction was quenched by immersing the NMR tube containing the sample in an ice-water bath. ^{1}H or ^{13}C NMR spectra were recorded after thawing.

2.4. Procedures for in situ NMR studies on fructose dehydration in DMSO-d_6 with 0.5% $H_2{}^{17}O$

A solution of D-fructose (15 mg) and 1.3 mg of Amberlyst 70 (or PO_4^{3-}/niobic acid) in 0.5 ml of DMSO-d_6 containing $H_2{}^{17}O$ (20.0 at% ^{17}O) was prepared in a 5-mm J-Young NMR tube. The tube was then transferred to a Varian Inova-400 NMR spectrometer where the ^{17}O NMR spectrum was recorded at room temperature. The NMR tube was then heated to 80 °C, and in situ ^{17}O NMR spectra were recorded at regular intervals for up to 24 h while keeping the temperature at 80 °C using conditions identical to the $t = 0$ spectrum.

2.5. Liquid chromatography–mass spectrometry (LC–MS) analysis of reaction mixtures

For the LC–MS experiments, similar procedures were employed and similar results were obtained for all three catalysts, Amberlyst 70, PO_4^{3-}/niobic acid and sulfuric acid. Amberlyst 70 is explicitly discussed as an example. A solution of 3 wt% fructose (0.903 g) in DMSO (30 ml) was heated at 80 °C for 8 h with the Amberlyst 70 (0.075 g). The reaction was then quenched by immersing the flask containing the sample in an ice-water bath. When PO_4^{3-}/niobic acid was used as a catalyst the contents were immediately centrifuged to separate the finely powdered catalyst from the reaction mixture. The clear portion of the solution, obtained by decanting, was diluted by H_2O to yield a final solvent mixture of 95% H_2O and 5% DMSO and filtered before ESI–MS analysis. A control experiment was performed with 30 mg fructose dissolved in 1.0 mL DMSO diluted with H_2O to make the final solvent mixture 95% H_2O and 5% DMSO, which was then filtered before ESI–MS analysis.

The LC–MS/MS system was an Aglient Technologies 1200 series HPLC coupled to an Agilent Technologies 6210 ESI TOF-MS mass spectrometer. A 5 μL aliquot of the solution was injected into the LC–MS/MS system. An Agilent poroshell 120 EC-C18 RPLC column, 30 × 50 mm size, 2.7 micron particle size, maintained at 60 °C, was used for analysis. The two mobile phases were 0.1% formic acid in water (solvent A) and 0.1% formic acid in acetonitrile (solvent B).

2.6. Theoretical methods

We have employed the highly accurate G4MP2 [43] level of theory to evaluate gas phase energetics of reaction intermediates at 298 K, similar to our previous studies of fructose [44–46]. The solvation energies were computed using the SMD [47] solvation model at the B3LYP/6-31G(2df,p) level of theory using the DMSO solvent (ε = 46.8). Initial starting geometries were taken from our previous studies [44,45]. Energies of selected geometries were computed with incorporation of explicit DMSO molecules in the model. A computed value of −264.4 kcal/mol ($3\,DMSO + H^+ \rightarrow H^+(DMSO)_3$, in implicit DMSO solvent) is taken as the Gibbs free energy of protonation of DMSO in computing the relative free energies of protonation and deprotonation in the DMSO medium. DMSO was treated as a discrete solvent in calculations involving species C1 (intermediate 1) and C2 since the experimentally observed structure of **Int. 1** (by NMR) corresponds to the theoretically predicted structure when the discrete solvent model is used. A continuum model is used in the treatment of all other species (including **Int. 2** and **Int. 3**). The NMR spectra of **Int. 3** matches that of the predicted spectra of the theoretically calculated species without invoking complexation with DMSO. **Int. 2** is not observed by NMR. All calculations were performed using Gaussian 09 software [48].

3. Results and discussion

In this report we present a molecular level investigation of the mechanism for the acid catalyzed triple dehydration of fructose to form HMF. Two heterogeneous catalysts, Amberlyst 70 and PO_4^{3-}/niobic acid as well as a homogeneous catalyst – sulfuric acid – were used in this study. Amberlyst 70 and sulfuric acid are both Brønsted acids, while PO_4^{3-}/niobic acid $^-$ has both Lewis and Brønsted acid sites [42]. The same intermediates are identified with any of the three catalysts. The intermediates are: 2-(hydroxydimethylsulfinyloxy)-β-D-fructofuranose (**Int. 1**), another species (**Int. 2**) capable of keto–enol tautomerism,4-dihydroxy-5-hydroxymethyl-tetrahydro-furan-2-carbaldehyde (the keto form)-2-(hydroxymethyl)-5-(hydroxylmethylene)-tetrahydrofuran-3,4-diol (the enol form) and 4-(hydroxy)-5-(hydroxymethyl)-4,5-dihydrofuran-2-carbaldehyde (**Int. 3**). This is the first report in the literature for **Int. 1**, while the enol form of **Int. 2** [40] and **Int. 3** [33,34,40], were previously reported. All intermediates were identified using ESI–MS. Additionally, **Int. 1,** a complex with the DMSO solvent was characterized by means of routine ^{13}C and ^{17}O NMR spectroscopic techniques as well as by NMR using ^{13}C enriched fructose and DEPT. **Int. 3** was characterized by means of ^{13}C NMR spectroscopy.

All three intermediates that have been identified experimentally correspond to local energy minima in the theoretically calculated potential energy landscape for the triple dehydration of fructose to form HMF. The keto from of **Int. 2** has a lower theoretically calculated potential energy (Section 3.8 below) than its enol form. However as will be discussed in more detail later, the energy barriers and preexponentials for reactions that lead to the formation and disappearance of an intermediate are also expected to influence the steady state concentration of any intermediate. The role of the solvent, DMSO, is also discussed. It was previously reported that the dehydration of fructose in DMSO with a PO_4^{3-}/niobic acid catalyst results in the formation of furfural in addition to HMF [41]. Furfural is not seen as a product with the other catalysts used in this study. It was demonstrated that furfural does not originate from HMF under reaction conditions. Thus, furfural is formed from fructose via a pathway accessed when PO_4^{3-}/niobic acid is the catalyst [41]. We hypothesize that the pathway for furfural formation, which is only observed in our study with a PO_4^{3-}/niobic acid catalyst, is a result of the Lewis acid sites that are reported to be present for PO_4^{3-}/niobic acid. Using IR spectroscopy and pyridine as a probe molecule, we verified that PO_4^{3-}/niobic acid $^-$ has both Lewis and Brønsted acidic sites (Supporting information, Fig. S1), analogous to what has been reported for niobic acid in the literature [42]. However, a more detailed investigation of the mechanism for furfural formation is beyond the scope of this report.

3.1. Role of solvent

The acid catalyzed dehydration of fructose has been reported in DMSO in high yield even in the absence of an added acid catalyst. As such, it has been suggested that in addition to being a solvent, DMSO also acts as the catalyst for this reaction [33]. However, DMSO decomposes at moderate temperatures (~80 °C) in the presence of oxygen to produce acidic species, including H_2SO_4 [35]. We present data to show that it is these acidic species, rather than the solvent itself, that catalyzes the dehydration reaction. We do this by carrying out the dehydration of fructose in DMSO in the absence of an added catalyst, both in presence of air and under an inert atmosphere. In the latter case, no evidence of either the intermediates or the final HMF product is seen after 24 h of reaction time, while in the former case the reaction proceeds along with formation of the intermediates to produce obvious HMF peaks in about 3 h reaction time at 100 °C. This behavior demonstrates that the decomposition of DMSO in presence of air into acidic species is the origin of its apparent catalytic behavior. The relevant spectra are presented in the Supporting information (Fig. S2).

However, DMSO does play a direct role in the overall reaction pathway. Theoretical calculations and experimental evidence demonstrate (Sections 3.8 and 3.3, respectively) that a key intermediate, **Int. 1,** identified in the reaction pathway is a complex that incorporates DMSO. Consistent with the involvement of solvent in the overall reaction, Kimura et al. [34] observe different products for the dehydration of fructose with different solvents-DMSO, water, and methanol.

The reaction of fructose in DMSO leads to reduction of humin formation compared to when the same reaction is carried out in

water. Horvath [40] suggested that the preference for 5-member rings in DMSO over 6-member rings in water is at least a contributory factor in this observation. As previously reported [41], the carbon balance we obtained in DMSO was at least 82% using Amberlyst 70 as a catalyst and at least 65% when using a PO_4^{3-}/niobic acid catalyst. In this study we determined that the yield of HMF with sulfuric acid could exceed 80% at a number of temperatures and acidities. There yields were determined based on a comparison of the HMF signal to that of a calibrated HMF standard solution at a time after all the starting fructose had reacted. Humins, soluble polymers, and other byproducts that formed were not analyzed in detail in this work. It is also relevant to mention that the rehydration of HMF to form levulinic acid and formic acid is effectively inhibited when working in DMSO since this reaction requires added water [41].

3.2. Observation of the intermediates in the dehydration of fructose in DMSO-d_6 by ^{13}C NMR

In this study, we focus on information relevant to the molecular level mechanism for HMF formation from fructose in DMSO. Fig. 1 shows a time-progression of ^{13}C NMR spectra for the dehydration of D-fructose in DMSO-d_6 with an Amberlyst 70 catalyst at 80 °C. During the first 2 h the spectra show mainly the four cyclic tautomers of fructose [49,50]. Six new carbon resonances at 57.4, 65.6, 78.1, 81.0, 82.4, and 108.0 ppm are observed at approximately t = 1 h, indicating the formation of a reaction intermediate, which we denote as **Int. 1**. The ^{13}C NMR spectra for reaction times beyond 2 h show an increase in the peaks corresponding to **Int. 1**. The ^{13}C NMR spectra, taken at t = 1 also confirm the production of an HMF product with resonances at 56.5, 110.0, 124.6, 151.8, 162.0, and 178.3 ppm, which are consistent with the reported ^{13}C chemical shifts for HMF [51]. The ^{1}H NMR spectra (not shown) of this sample further confirmed the production of HMF with the peaks at 4.50 (s), 6.60 (d, J = 3.6 Hz), 7.38 (d, J = 3.6 Hz), and 9.49 (s) ppm.

At t = 8 h, the amplitude of the signal due to HMF has increased, whereas beyond t = 5 h the amplitude of the resonances due to **Int. 1** decrease with an increase in the HMF signal. Finally, the signal due to **Int. 1** is no longer visible at t = 24 h and the amplitude of the HMF resonances have further increased to close to their final level. Careful examination of the ^{13}C NMR spectra between t = 2 and t = 10 h, shows that a new set of resonances, three in the aliphatic region at 61.1, 90.1, 73.4 ppm, two in the alkene region at 122.5 and 156.4 ppm, and one in the carbonyl region at 184.0 ppm, appear and correspond to the another intermediate (**Int. 3**). As shown below (Section 3.5), evidence of another intermediate, **Int. 2,** is obtained from high resolution MS data. As also discussed below, and as is clear from the structures of **Int. 2** and **Int. 3**, the formation of **Int. 2** preceded the formation of **Int. 3** along the reaction pathway from fructose to HMF. Thus, to be consistent in naming the intermediates formed as this reaction progresses, we label the second intermediate observed via NMR as **Int. 3,** since it is the third intermediate based on progress along the reaction coordinate. From Fig. 1, it is clear that the intensity of NMR peaks assigned to **Int. 3** increase when the reaction time increases from 2 to 6 h. When the reaction time reaches 7 h the intensity of the resonances associated with **Int. 3** begin to decrease until they are barely visible at t = 12 h. No signals due the levulinic acid or formic acid rehydration products were observed in either the ^{13}C or ^{1}H NMR spectra under these conditions. ^{13}C spectra demonstrate that there are separate sets of six resonances that appear for **Int. 1** and **Int. 3**, respectively. To confirm that each set of six resonances are assigned to a single intermediate, we monitor the changes in the normalized intensity of the NMR resonances assigned to **Int. 1** and **Int. 3** during the reaction. Fig. 2 shows the ^{13}C NMR spectrum for the fructose dehydration catalyzed by sulfuric acid at 83 °C carried out under a N_2 atmosphere. Fig. 2a (bottom) clearly shows all the six resonances assigned to **Int. 1** at 57.4, 65.6, 78.1, 81.0, 82.4, and 108.0 ppm and none of the resonances assigned to **Int. 3**. However after 22 min (Fig. 2 (top)) six new resonances appear at 61.1, 90.1, 73.4, 122.5, 156.4 and 184.0 ppm that we had earlier attributed to **Int. 3**. It may also be noted that the normalized intensity of each of the resonances that were assigned to **Int. 1** has approximately doubled during this time interval (Supporting information, Table S1). The fact that the time dependence of the amplitude of all 6 resonances assigned to **Int. 1** is essentially the same is consistent with their assignment to a single species. The resonances due to **Int. 3** are not observable at 12.5 min of reaction time. Thus, their amplitude must increase by much more than a factor of two in going from 12.5 to 22 min. If any of the resonances assigned to **Int. 1** actually belonged to **Int. 3** their amplitude would increase much more than a factor of 2 between 12.5 and 22 min of reaction time. The fact that this does not happen is consistent with our assignments of resonances to **Int. 1** and **Int. 3,** respectively. To further support our assignment, each of the set of resonances was monitored as the reaction progressed and it was found that the six carbon resonances due to **Int. 1** change in parallel with each other as do the six carbon resonances assigned to **Int. 3**. The relevant data for Amberlyst 70 and PO_4^{3-}/niobic acid are presented in the supporting information (Figs. S2 and S3, respectively). This behavior is also consistent with the six peaks assigned to **Int. 1** being due to a single species with the same behavior and same conclusion for **Int. 3**. The reactions of fructose in DMSO-d_6 using PO_4^{3-}/niobic acid at 80 °C (Fig. S5) and Amberlyst 70 at 100 °C (Fig. S6) were also studied. Dehydration reactions under an inert atmosphere catalyzed by sulfuric acid at 100 °C were also carried out (Fig. S7). In each case, based on both ^{13}C and ^{1}H NMR spectra, **Int. 1** and **Int. 3** are also observed, consistent with the same mechanism for the triple dehydration of fructose being operative for any of the catalysts used. Fig. 3a shows the changes in the normalized intensity for the ^{13}C NMR signals from fructose, **Int. 1**, **Int. 3**, and HMF, during the course of the reaction using Amberlyst 70 as the catalyst at 80 °C. The normalized intensities were determined using a biphenyl internal standard. In Fig. 3a, **Int. 1, Int. 3** and HMF can be seen at t = 1 h, with their yields increasing with increasing reaction time. The concentration of **Int. 1** starts to decrease at ~5 h and is no longer visible at 16 h, while **Int. 3** is barely detectable at t = 12 h. Fig. 3b shows the analogous result using PO_4^{3-}/niobic acid as catalyst at 80 °C. There appear to be some differences in the relative shapes of the traces with the two catalysts (Fig. 3) including that the presence of induction times are easier to see in the kinetic profile obtained with PO_4^{3-}/niobic acid than with Amberlyst 70 (Fig. 3a) as the catalyst. Differences in acidity could be responsible for and/or contribute to the differences in signal shape when using niobic acid versus Amberlyst 70 as catalysts. Preliminary data from our group indicates that the rate of reaction of fructose to form HMF depends on acidity. In addition, it is possible that the different catalysts could differentially affect the rates of specific steps in the overall reaction mechanism. In Fig. 3b, **Int. 1** can be seen at t = 2 h, while **Int. 3** is first observed at approximately 4 h. After 5 h, signals due to HMF become apparent, with the HMF yield increasing with increasing reaction time. The concentration of **Int. 1** starts to decrease at ~6 h and is no longer visible at 16 h, while **Int. 3** is barely detectable at t = 10 h. Another noteworthy feature of both of the above reaction profiles (Fig. 3a and b) is that during the initial time periods (0–5 h) it is clear by visual inspection that the rate of rise of the curve for **Int. 1** is faster than the rate of rise of the curve from **Int. 3**. This also provides further evidence that the production of **Int. 1** indeed precedes the production of **Int. 3**.

There are several mechanistic investigations of the reaction of fructose that report on the structure of observed intermediates [11,36–39,52]. As an initial step in the determination of the

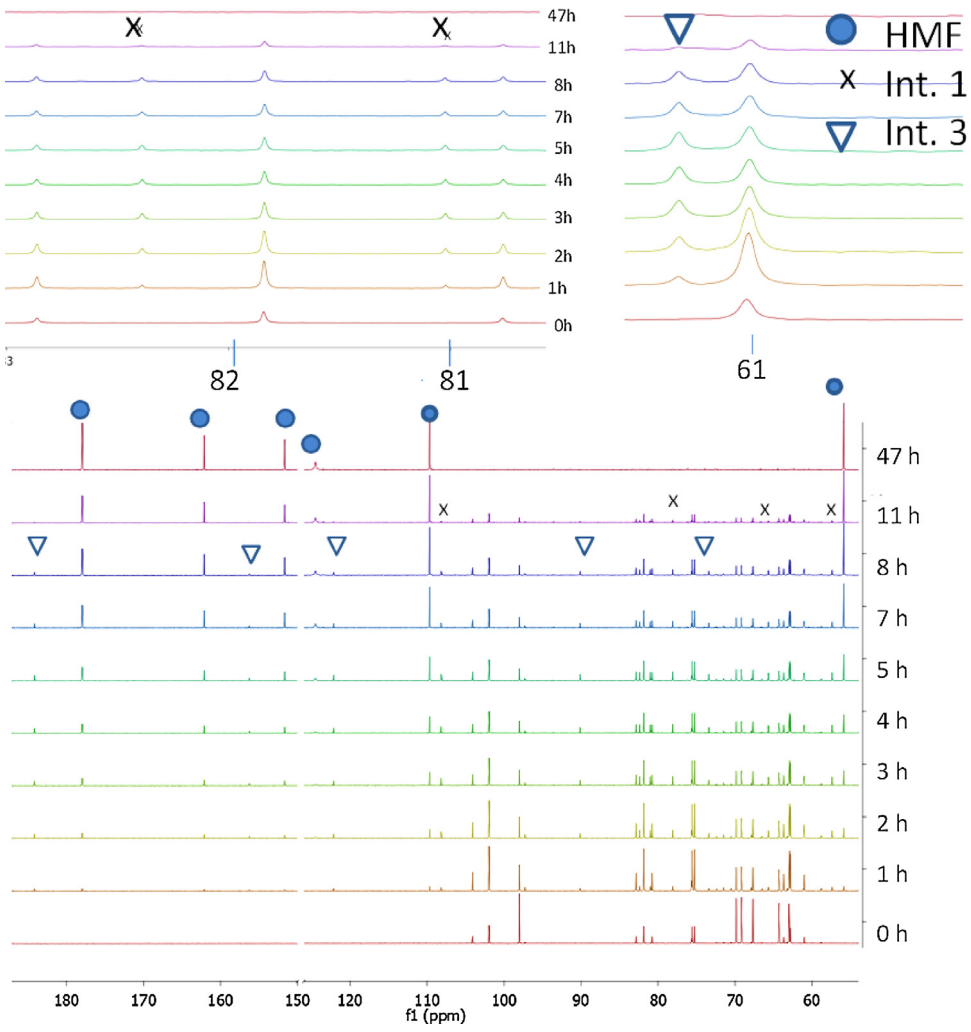

Fig. 1. ^{13}C NMR spectra for the dehydration of D-fructose in DMSO-d_6 using Amberlyst 70 as catalyst at 80 °C.

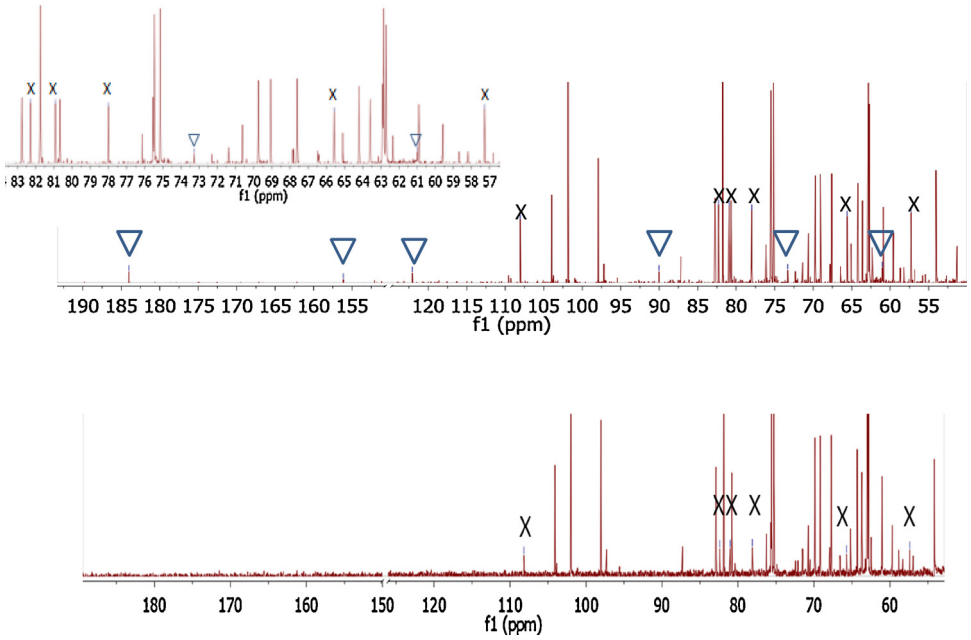

Fig. 2. The resonances of **Int. 1** and **Int. 3** after 12.5 min (bottom) and 22 min (top). The reaction was carried out under an inert atmosphere at 83 °C using sulfuric acid as the catalyst.

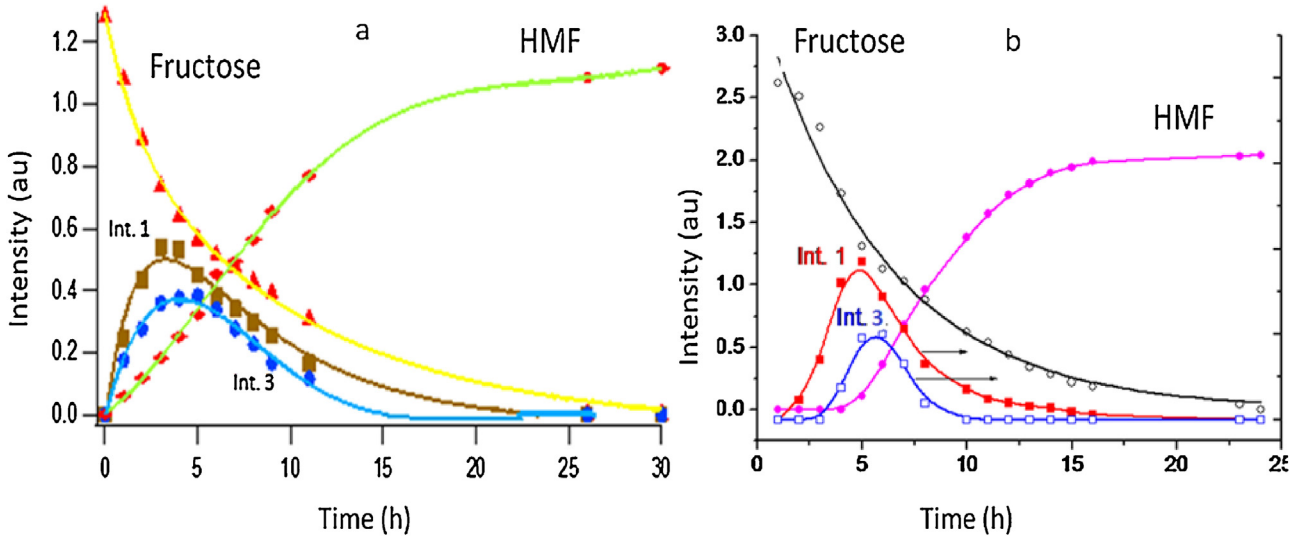

Fig. 3. Changes in the normalized intensity of D-fructose, HMF, **Int. 1**, and **Int. 3** during the reaction (3 wt% of D-fructose in DMSO-d_6 catalyzed by (a) Amberlyst 70 and (b) PO_4^{3-}/niobic acid at 80 °C). The normalized intensities were determined using the biphenyl internal standard.

structures of **Int. 1** and **Int. 3**, we attempted to predict the NMR resonances (Using Modgraph NMRPredict as part of MestReNova 6.0.2) of the intermediates proposed in the literature, and of the calculated low energy intermediates described in Section 3.8. The NMR peaks of **Int. 1** (57.4, 65.6, 78.1, 81.0, 82.4, and 108.0 ppm) do not match any of the intermediates proposed in the literature for either the cyclic pathway or open-chain pathway. The relation of the experimentally characterized structures to the structures of the calculated intermediates will be discussed in Section 3.8.

However, the NMR resonances of **Int. 3** (61.1, 90.1, 73.4, 122.5, 156.4, and 184.0 ppm) compare well to the chemical shifts of a reported cyclic intermediate, 4-(hydroxy)-5-(hydroxymethyl)-4,5-dihydrofuran-2-carbaldehyde (Table 1), with resonances reported at 122.8, 156.8, and 184.9 ppm for fructose dehydration to HMF in DMSO-d_6 at 150 °C in the absence of a catalyst [33]. Since this reaction was carried out in the presence of air at a high temperature, we expect that it was catalyzed by acidic species, including H_2SO_4 [33]. Corresponding resonances were reported at 61.3, 73.6, 90.3, 122.3, 156.4, and 184.3 ppm for fructose dehydration with a H_2SO_4 catalyst in DMSO at 120 °C [40]. The same structure as **Int. 3** was reported by Kimura [34] with the ^{13}C resonances observed at 62, 90, 85, 129, 157 and 186 ppm.

3.3. Structural analysis of the intermediates using DEPT spectra

To further investigate the structures of **Int. 1** and **Int. 3**, distortionless enhancement of NMR signals by polarization transfer (DEPT) was used to determine the number of protons on each carbon atom. DEPT spectra were obtained at $\theta_z = 135°$ where CH and CH_3 appear in a phase opposite to the phase CH_2 appears in. Fig. 4 shows the DEPT 135 spectrum at $t = 6$ h, which has the —CH_2 peaks at 57.4 and 65.6 ppm and the —CH peaks at 78.1, 81.0 and 82.4 ppm for **Int. 1**. For **Int. 3**, the DEPT 135° spectrum gives the —CH_2 peaks at 61.1 ppm and the —CH peaks at 73.4, 90.1, 122.5, and 184.0 ppm. The carbon resonances that are recorded using ^{13}C NMR but are absent in DEPT are carbons without any attached hydrogen. The types of carbons in **Int. 3** match well with the respective carbon types in -4-(hydroxy)-5-(hydroxymethyl)-4,5-dihydrofuran-2-carbaldehyde (Table 1).

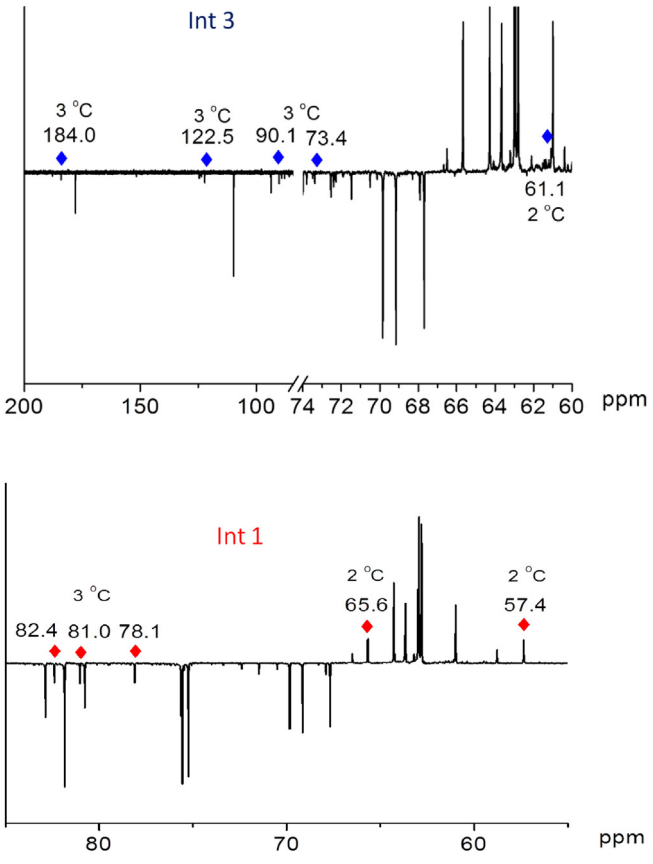

Fig. 4. The DEPT 135 ^{13}C NMR spectrum at $t = 6$ h for the D-fructose dehydration reaction at 80 °C in DMSO-d_6 with Amberlyst 70 catalyst. (a) ^{13}C NMR spectra between 85 and 200 ppm, (b) ^{13}C NMR spectra between 55 and 85 ppm.

3.4. Structural analysis of the intermediates using ^{13}C labeled D-fructose

Experiments were performed to determine where the ^{13}C label at the C-1, C-2, and C-6 carbons in fructose resides in the intermediates and the HMF product. The numbering scheme employed

Table 1
NMR data for 4-hydroxy-5-hydroxymethyl-4,5-dihydrofuran-2-carbaldehyde **(Int. 3)**.

	Int. 3					
Origin of carbon	C^1	C^2	C^3	C^4	C^5	C^6
δ_C/ppm (experimentally observed)	184.0	156.4	122.5	73.4	90.1	61.1
Chemical shift/ppm (predicted)	187.0	160.6	122.9	75.4	86.2	62.2
Type of carbon	1°	4°	1°	1°	1°	2°
δ_H/ppm	9.47 (s)	–	6.25 (d)	4.81 (dd)	4.26 (td)	3.46 (m)

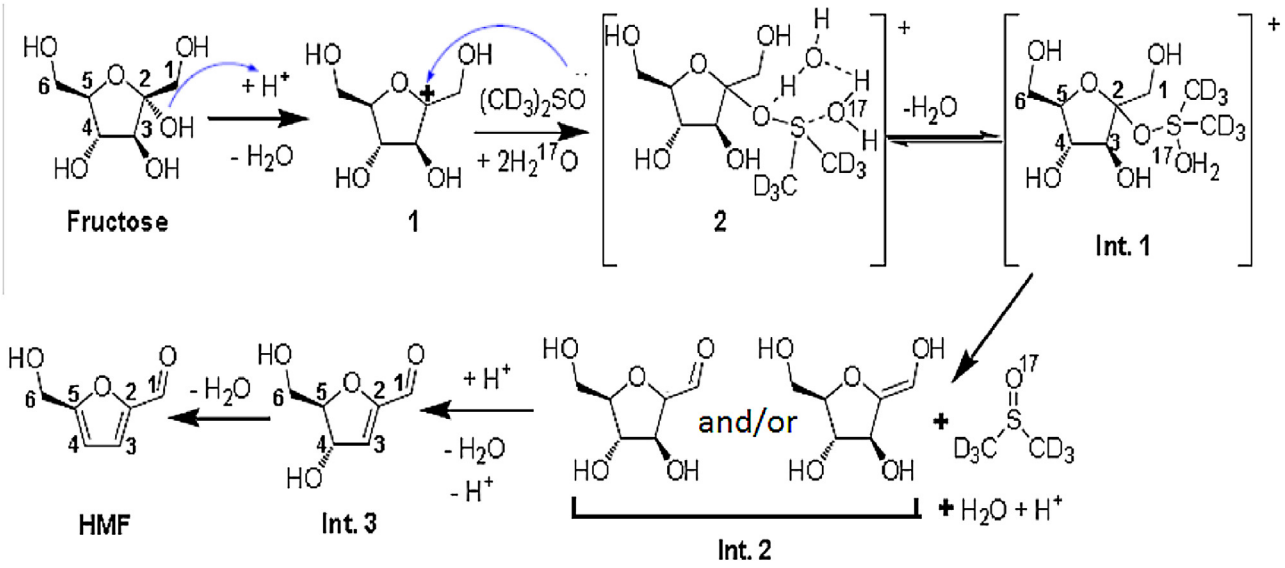

Scheme 2. A proposed schematic mechanism for the catalytic conversion of fructose to HMF in DMSO.

is depicted in Scheme 2. The Scheme also depicts a plausible pathway for the overall reaction, but not necessarily a unique one. These results are displayed in Fig. 5, as a function of reaction time, at 80 °C in DMSO-d_6, using an Amberlyst 70 catalyst.

The initial spectrum (t = 0 h) in Fig. 5 demonstrates that the NMR signals at 97.3, 98.1, 102.0, 104.1, and 213.9 ppm, due to the C-2 carbon in the five tautomers of fructose (α-furanose, β-furanose, β-pyranose, α-pyranose, and open-chain fructose), are enhanced due to ^{13}C enrichment. Spectra taken at 1 h indicate that the intensity of the peak at 108.0 ppm, which belongs to the **Int. 1**, is enhanced relative to the intensities of other **Int. 1** NMR peaks. Thus, the C-2 carbon of fructose is the origin of the 108.0 ppm peak of **Int. 1**. The peak at 108.0 ppm becomes readily apparent after 2 h, and a resonance at 156.4 ppm attributed to **Int. 3** is evident for a reaction

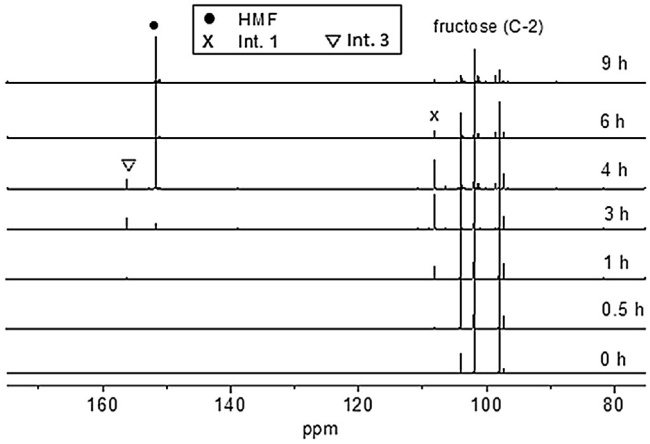

Fig. 5. ^{13}C NMR spectra for the dehydration of [^{13}C-2] fructose in DMSO-d_6 using Amberlyst 70 as the catalyst at 80 °C.

time of ~3 h. After 4 h of reaction time the resonance at 154.5 ppm, which is due to the C-2 carbon in HMF, is enhanced greatly. The two resonances at 108.0 and 156.4 ppm decrease in intensity after 6 h. However, the resonance at 154.5 ppm increases in intensity with increasing reaction time. The peaks at 108.0 and 156.4 ppm have greatly diminished in intensity and are barely visible at t = 9 h, and the ^{13}C NMR spectrum is dominated by the HMF resonances. These results indicate that C-2 of fructose ends up producing the 108.0 ppm resonance for **Int. 1** and then the 156.4 ppm (C-2) signal of **Int. 3**, and finally ends up as the C-2 (154.5 ppm) carbon of HMF.

When [^{13}C-1] fructose was used as precursor (at 80 °C, using Amberlyst 70), the intensity of the resonances at 57.4 and 184.0 ppm, are enhanced relative to the intensities of other **Int. 1** and **Int. 3** NMR peaks respectively, which are too weak to be visible in Fig. S8. Thus, the C-1 carbon of fructose is the origin of the 57.4 and 184.0 ppm (C-1) resonances of **Int. 1** and **Int. 3** respectively. Furthermore, a peak in the carbonyl region at 178.3 ppm, assigned to the aldehyde carbon (C-1) in HMF, is greatly enhanced. This latter result indicates that C-1 carbon of fructose remains in the C-1 position in HMF. Using [^{13}C-6] fructose (Fig. S9) under the same conditions as indicated above, ^{13}C NMR data indicates that the C-6 carbon of fructose maps onto the 65.6 ppm resonance in **Int. 1** (C-6) and the 61.1 ppm resonance (C-6) in **Int. 3**. Moreover, the C-6 carbon of fructose is the origin of the C-6 carbon of HMF, which is in agreement with our previous results [41].

We note that the experiments involving ^{13}C enriched fructose were carried out in a sealed J-Young tube while batch reactions were carried out in open reaction vessels (unless otherwise noted). As a result of these differences in reaction conditions the time dependence of the temperature the sample was exposed to, and potentially the degree of exposure to air for the two samples were different. Both exposure to air and the time at elevated temperature can affect the acidity of the DMSO solution and thus the rate of reaction. The major focus of this work was identification of

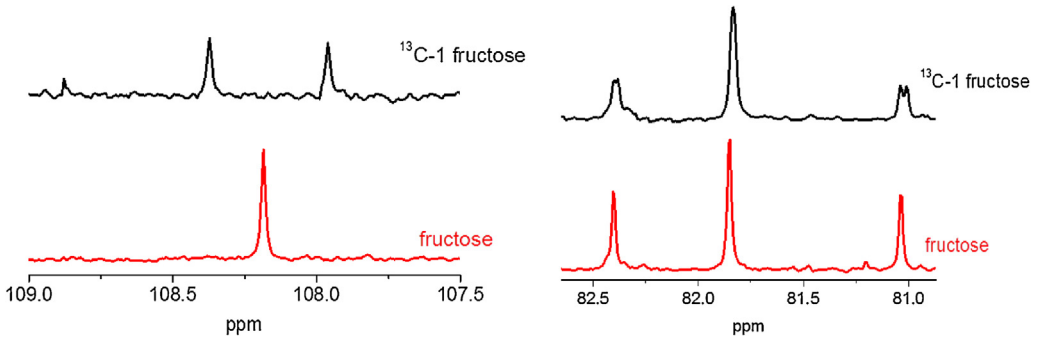

Fig. 6. Comparison of the ^{13}C NMR peaks at 81.0, 82.4, and 108.0 ppm when [^{13}C-2] fructose and fructose, respectively, were used as precursors for the dehydration reaction in DMSO-d_6 using an Amberlyst 70 catalyst.

intermediates using different catalysts. A quantitative study of the kinetics of these reactions was beyond the scope of this work. However, the order, of appearance of Int. 1, Int. 2 and Int. 3 and HMF is the same under both sets of conditions. In addition, since niobic acid and Amberlyst 70 are solids, a quantitative study of the kinetics of the reaction of fructose with these catalysts would be challenging. ^{13}C—^{13}C coupling parameters provide direct information about the connectivity of the skeleton of the intermediates [53,54]. As discussed above, the reaction of [^{13}C-1] fructose, leads to a strong ^{13}C resonance at 57.4 ppm in **Int. 1** and at 184.0 ppm in **Int. 3**. Careful inspection of other NMR peaks due to **Int. 1** shows that three natural-abundance signals (81.0, 82.4, and 108.0 ppm) are split into doublets (Fig. 6), directly giving the coupling constant, J_{CC}, with the labeled C-1 carbon which are presented in Table 2. For comparison, the signals at 81.0, 82.4, and 108.0 ppm when unlabeled fructose is used as precursor are also shown in Fig. 6.

As shown in Table 2, for [^{13}C-1] fructose, the coupling constants for the NMR resonances at 81.0, 82.4, and 108.0 ppm in **Int. 1** are 3.8, 2.5, and 51.5 Hz, respectively. The large one-bond ^{13}C—^{13}C spin-coupling constant of 51.5 Hz indicates that the resonance at 108.0 ppm is due to the carbon adjacent to the labeled site and is thus attributed to C-2 in **Int. 1**. The resonances at 156.4, 122.5, 73.4, and 90.1 ppm attributed to **Int. 3** obtained from [^{13}C-1] fructose were each split into a doublet and the corresponding coupling constants are 60.4, 9.3, 1.8, and 4.3 Hz (Table 2). The large one-bond ^{13}C—^{13}C spin-coupling constant of 60.4 Hz indicates that the resonance at 156.4 ppm is adjacent to the labeled site (C-1) and thus attributed to the C-2 carbon in **Int. 3**.

Other one-bond (^{1}Jcc) and longer-range ^{13}C—^{13}C spin-couplings (e.g., ^{2}Jcc, ^{3}Jcc, etc.) were obtained from analysis of the ^{13}C NMR spectra of the reactions of [^{13}C-2] fructose and [^{13}C-6] fructose (Table 2). When [^{13}C-6] fructose was used as the precursor the ^{13}C NMR spectrum gives an enhanced peak at 65.6 ppm and a doublet at 82.4 ppm with a 33.1 Hz coupling constant for **Int. 1**. This indicates that the peak at 82.4 ppm carbon is adjacent to C-6 (65.6 ppm peak) in **Int. 1.** Moreover, the only ^{13}C—^{13}C spin-coupling between C-6 and other carbons in **Int. 1** involves the resonance at 82.4 ppm (Table 2), indicating that there is no other carbon adjacent to C-6 except this one.

With [^{13}C-2] fructose as the reactant, three resonances, at 184.0, 122.5, and 90.1 ppm, appear as doublets with 72.3, 60.3, 2.6 Hz coupling constants, respectively (Table 2). Again, the large ^{13}C—^{13}C spin-coupling constants of 72.3 and 60.3 Hz, for the resonances at 184.0 and 122.5 ppm indicate that these resonances are due to carbons adjacent to the labeled (C-2) site and are thus attributed to the C-1 and C-3 carbons in **Int. 3**. As seen above, using a [^{13}C-1] fructose reactant, the resonance at 184.0 ppm is attributed to C-1 in **Int. 1**, thus the resonance at 122.5 ppm is attributed to the C-3 carbon in **Int. 3**.

The connectivity of the carbon skeleton of **Int. 1** can be deduced based on the magnitudes of the one bond and longer range J_{CC} coupling constants. The C-1, C-2, and C-6 carbons of fructose produce the resonances seen at 57.4, 108.0, and 65.6 ppm in **Int. 1** that end up as the C-1, C-2, and C-6 carbon in **Int. 3,** and finally end up as the C-1, C-2, and C-6 carbon in HMF respectively. Therefore, the fructose dehydration reaction does not appear to involve C—C bond cleavage. Additionally, based on coupling constants (Table 2) we can conclude that the resonances at 81.0, 78.1, 82.4 ppm can be attributed to C-3, C-4, and C-5 carbons, respectively, in **Int. 1.**

These results from DEPT spectra and ^{13}C labeling are all consistent with **Int. 3** being identified as 4-(hydroxy)-5-(hydroxymethyl)-4,5-dihydrofuran-2-carbaldehyde. The structure of **Int. 1** is discussed in Section 3.7 below.

Table 2
$^{n}J_{CC}$ coupling constants (in Hz) in **Int. 1** and **Int. 3**.

Int. 1			**Int. 3**		
^{13}C-labeled position	δ_C/ppm	J_{CC}/Hz	^{13}C-labeled position	δ_C/ppm	J_{CC}/Hz
1	57.4	51.5(C1-C2) 3.8(C1-C3) 2.5(C1-C5)	1	184.0	60.4(C1-C2) 9.3(C1-C3) 1.8(C1-C4) 4.3(C1-C5)
2	108.0	51.1(C1-C2) 44.4(C2-C3)	2	156.4	60.3(C1-C2) 72.4(C2-C3) 2.7(C2-C5)
3	81.0	-	3	122.5	-
4	78.1	-	4	73.4	-
5	82.4	-	5	90.1	-
6	65.6	33.1(C5-C6)	6	61.1	42.3(C5-C6) 2.0(C4-C6)

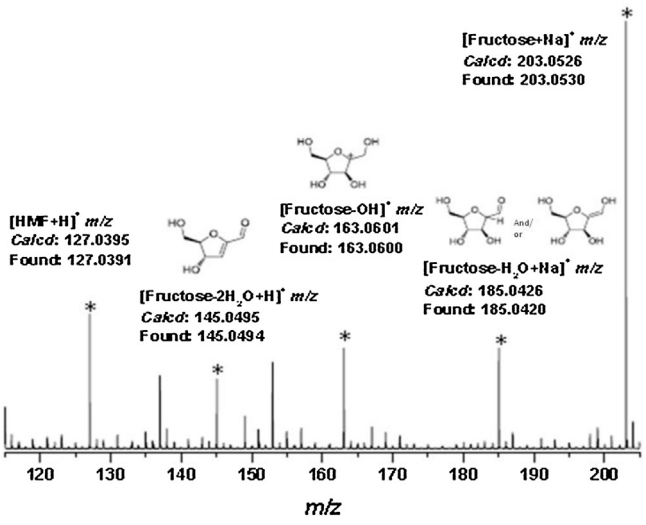

Fig. 7. ESI Mass spectrum of the reaction mixture for fructose in DMSO using an Amberlyst 70 catalyst at 80 °C after 6 h.

3.5. Structural analysis of the intermediates: High resolution electrospray ionization mass spectrometry (HR ESI–MS)

To further probe the structure of the intermediates, a mixture of fructose in DMSO with the Amberlyst 70 catalyst, that had been allowed to react at 80 °C for 6 h, was subjected to HR ESI–MS analysis. The mass spectrum, shown in Fig. 7, revealed five peaks at mass-to-charge (m/z) ratios of 127.0391, 145.0494, 163.0600, 185.0420, and 203.0530, corresponding to $[C_6H_7O_3]^+$ ($[HMF+H]^+ = [Fructose - 3H_2O + H]^+$), $[C_6H_9O_4]^+$ ($[Fructose - 2H_2O + H]^+$), $[C_6H_{11}O_5]^+$ ($[Fructose - OH]^+$), $[C_6H_{10}NaO_5]^+$ ($[Fructose - H_2O + Na]^+$), and $[C_6H_{12}NaO_6]^+$ ($[Fructose + Na]^+$), respectively. These peaks were isotopically resolved and match very well with the theoretical mass spectra for the indicated compounds predicted by the Agilent MassHunter software. Some higher mass number peaks were also observed and are attributed to humin-like polymers. LC was used to separate out higher mass species from the species shown in Fig. 7.

As a control, ESI–MS analysis was also performed for a sample of fructose dissolved in DMSO at room temperature in the absence of a catalyst. Peaks at m/z of 145.0494, 163.0600, and 185.0420, were observed for the reacting system, and were not observed in the ESI–MS of the control sample. These results indicate that the above three mass peaks originate from three species produced during the acid catalyzed fructose dehydration reaction taking place in DMSO. The structures of the relevant fragment ions are also shown in Fig. 7. The same three species are obtained with ESI–MS for the fructose dehydration reaction in DMSO in presence of PO_4^{3-}/niobic acid catalyst, sulfuric acid or in presence of air without an added acid catalyst. The peaks at m/z 163.0600, 185.0420 and 145.0494 correspond to **Int. 1**, **Int. 2** and **Int. 3**, respectively.

3.6. Structural analysis of the intermediate 1: ^{17}O NMR data

To obtain additional information about the structure of **Int. 1**, the fructose dehydration reaction was carried out in DMSO-d_6 containing 0.5% $H_2{}^{17}O$, and the reaction was monitored by in situ ^{17}O NMR. Fig. 8a displays the in situ ^{17}O NMR spectra obtained during the reaction of fructose in DMSO-d_6 containing $H_2{}^{17}O$ at 80 °C using Amberlyst 70 as the catalyst. The signal at 0.0 ppm is due to the $H_2{}^{17}O$, while the peak at 12.4 ppm at $t = 0$ h is due to naturally occurring ^{17}O in the DMSO-d_6 solvent (Fig. 8b) [55]. Corresponding results are obtained when the reaction is carried out using PO_4^{3-}/niobic acid or without an added catalyst but in presence of air.

As seen in Fig. 8a, a peak at 60 ppm is observed at $t = 2$ h. In addition, the in situ ^{17}O NMR spectrum at $t = 2$ h confirmed the production of HMF with a peak at 582 ppm, which is a result of exchange between the aldehyde oxygen in HMF and $H_2{}^{17}O$. An increase in the characteristic resonances associated with HMF is accompanied by a decrease in the intensity of 60 ppm peak as the reaction proceeds from 2 h to 8 h. This result indicates that the peak at 60 ppm is due to a reaction intermediate. The time-scale for its appearance and disappearance indicates that this moiety corresponds to **Int. 1**. After 8 h the signal at 60 ppm has almost completely disappeared and the NMR peak due to HMF is dominant.

Additionally, the peak at 12.4 ppm (initially due to the naturally occurring ^{17}O in the DMSO-d_6) increases with the reaction time, indicating that ^{17}O is incorporated into the DMSO-d_6. The control experiment using $H_2{}^{17}O$ (0.5%) in DMSO-d_6 carried out in the absence of fructose, under the same experimental conditions, shows that the oxygen atom in DMSO-d_6 does not undergo exchange with $H_2{}^{17}O$ at 80 °C. Thus, the ^{17}O must be incorporated into DMSO as a result of DMSO participating in the dehydration reaction.

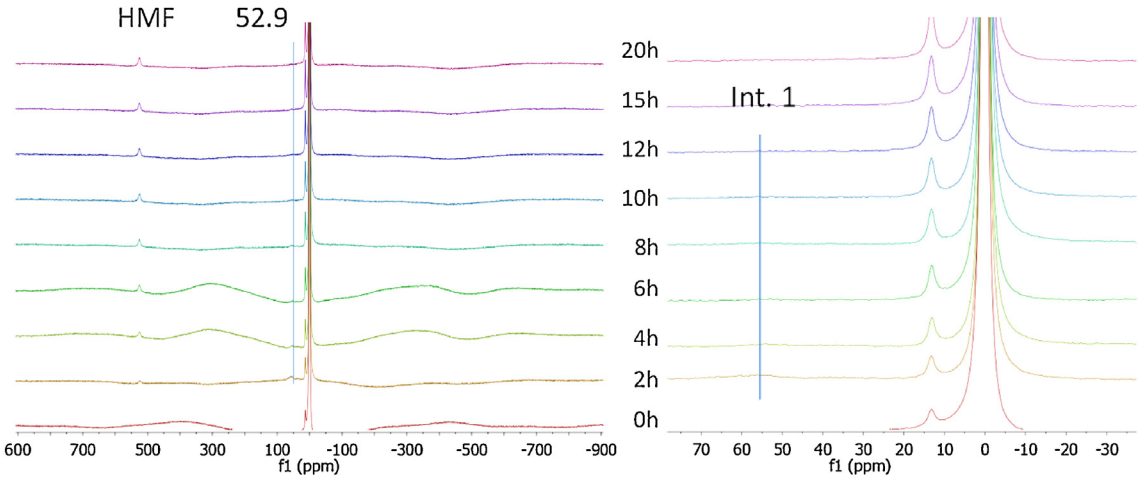

Fig. 8. In situ ^{17}O NMR spectra for the fructose reaction in DMSO-d_6 with added $H_2{}^{17}O$ (0.5%) at 80 °C using Amberlyst 70 as the catalyst.

3.7. Summary of the proposed reaction scheme based on experimental data

Data in the literature suggests that a furanose tautomer [11] is the gateway species through which fructose enters the reaction sequence delineated in Scheme 2. Combining the results from NMR and ESI–MS has allowed us to develop a common schematic reaction mechanism, Scheme 2, for the fructose dehydration reaction taking place in DMSO with a PO_4^{3-}/niobic acid, sulfuric acid, Amberlyst 70 catalyst, or without an added catalyst but in the presence of oxygen. The results of the ESI–MS study indicate that complexation of a carbo-cationic intermediate (**1**) by DMSO-d_6 to give a oxosulfonium intermediate (**2**) that incorporates a molecule of the DMSO solvent as well as two water molecules. MS results confirmed the formation of (**1**) as the m/z peaks at 163.0600 matches quite well with the calculated values of 163.0601. Oxosulfonium intermediates in mesylate reactions taking place in DMSO-d_6 that are similar to **2** have been characterized spectroscopically by Creary et al. [55] Horvath [40] has proposed the formation of fructosyl oxocarbenium ions as transition states which do involve complexation with the solvent. Our proposed structure for **Int. 1** is confirmed by ^{17}O labeling experiments, that indicate that the incorporation of ^{17}O in DMSO involves the formation of species **2** in Scheme 2 which in turn results from complexation of **1** with DMSO-d_6 as well as two $H_2{}^{17}O$ molecules. The resultant species (**2**) then loses a water molecule resulting in the formation of **Int. 1**. The loss of the solvent molecule leads to **Int. 2** and the incorporation of the ^{17}O label into DMSO-d_6. However, we note that since barriers to reaction have not been experimentally reported or calculated the data presented in this study does not preclude other reaction pathways such as the generation of Int. 1 from fructose and a parallel pathway for the generation of Int. 2 from fructose with the reaction progressing to form Int 3 and subsequently HMF.

Int. 1 could then break down to give the keto/enol intermediate (**Int. 2**) with an m/z = 185.0420, which has been identified in our ESI–MS data; 2-(hydroxymethyl)-5-(hydroxylmethylene)-tetrahydrofuran-3,4-diol (enol form), or 4-dihydroxy-5-hydroxymethyl-tetrahydro-furan-2-carbaldehyde (the keto form). The observed m/z matches quite well with the calculated m/z of 185.0426 expected for this intermediate. However, it is not possible to distinguish between the keto form and enol forms of this intermediate based on MS data. We note that the enol form of **Int. 2** was reported by Kimura et al. [34]. They proposed that the structure of the intermediate is a diol based on the absence of alkene peaks in the ^{13}C NMR spectra. Horvath [40] was able to detect **Int. 2** by means of NMR spectroscopy, and the enol structure was proposed in that report with assignments provided for the observed NMR resonances. However, we have not been able to detect either form of **Int. 2** by means of NMR spectroscopy. This suggests that under our reactions conditions, which involve a lower temperature for reaction than Horvath's study, there is a relatively low steady state concentration of **Int. 2** resulting from the rate of reaction of **Int. 2** significantly exceeding its rate of production.

In Scheme 2, the structure of **Int. 3** is consistent with the structure of the intermediate reported by Amarasekara, Horvath, and Kimura [33,34,40]. The m/z peak at 145.0494 that corresponds to **Int. 3** matches quite well with the calculated value of 145.0495, supporting this assignment. In the present study (as seen in Section 3.2), and in the work reported by Horvath [40], two sets of NMR resonances are observed and assigned to intermediates, **Int. 1** and **Int. 3**. Our assignment of the structure of **Int. 3** agrees with that previously reported [33,34,40]. All three studies propose a very similar set of steps from fructose to HMF. However, in Horvath's work **Int. 1** is identified as 2,6-anhydro-β-D-fructofuranose and they propose a mechanism for fructose dehydration that does not explicitly involve the solvent. Our results from the ^{17}O labeling studies and results from high-level quantum chemical methods, which are discussed below (Section 3.8), suggests that DMSO is involved in the formation of **Int. 1**, (the fructofuranosyl oxocarbenium ion), which may be in equilibrium with the 2,6-anhydro-β-D-fructofuranose in the presence of DMSO in an acidic medium. In Horvath's report, dehydration reactions were carried out at 120 °C and in Amarasekara's [33] report the reaction temperature was 150 °C. Our reaction conditions involve lower temperatures of 80–100 °C. It is possible that differences in reaction conditions could account for the reported differences in observations with regard to **Int. 1**.

As seen in Section 3.4 our experiments involving isotopically labeled C-13 precursors indicate that the position of the labels in the products is identical to that in the starting materials. This lack of scrambling of the labels indicate a lack of C—C bond cleavage in the tautomers of fructose as well as its successive dehydration products along the reaction coordinate to form HMF.

Finally, we note that the two heterogeneous catalysts used have different surface areas, thus mass transfer effects could conceivably play a role, however while these effects could lead to changes in the observed kinetics of the reaction they would not be expected to have an effect on the mechanism. Thus, the intermediates that we observe and the qualitative aspects of the kinetics remain the same with the different catalysts.

3.8. Computational study of the mechanism of the fructose dehydration

In order to understand the thermodynamic landscape of the reactions in even more detail, free energy calculations were performed for the fructose-HMF pathway. A detailed free energy surface using the G4MP2 level of theory (at 298 K) is shown in Fig. 9. In the presence of acid, protonation occurs at the tertiary hydroxyl site of fructose due to the high proton affinity of the tertiary hydroxyl group compared to secondary or primary hydroxyl groups [45]. In aqueous medium, the protonation of tertiary hydroxyl groups is endergonic by 8 kcal/mol [45], while in DMSO this process (**A** → **B**) is endergonic by 12.5 kcal/mol. Upon protonation of the tertiary hydroxyl group, the water molecule becomes a good leaving group and the complete detachment of water is moderately exergonic from **B** (**B** → **C**, −2.4 kcal/mol). However, formation of $\mathbf{C_1}$ (−4.6 kcal/mol) and $\mathbf{C_2}$ (−0.4 kcal/mol) is significantly exergonic from the protonated fructose (B). Species C_1 is a positively charged species formed by the complexation of oxycarbenium ion with DMSO and a water molecule (detached from the tertiary position). Complete detachment of a water molecule from $\mathbf{C_1}$ results in the formation of $\mathbf{C_2}$ (−0.4 kcal/mol).

Association and dissociation processes occurring in the gas phase result in significant changes in entropy contributions. However, these entropy effects are far less in solution, where solvent molecules (DMSO) are readily available to interact with solute and products. Since DMSO is only explicitly included in the first steps ($\mathbf{C_1}$ and $\mathbf{C_2}$) in Fig. 9, the entropy calculations for these species and subsequent intermediates must, by necessity, be treated differently. Therefore, the entropy contributions from the gas phase free energy calculation is not included in the formation of species $\mathbf{C_1}$ or $\mathbf{C_2}$ [56]. This approximation avoids a different treatment for these steps compared to the other intermediates for which an explicit complexation with a solvent molecule is not included.

One way leading to the formation of D is via removal of DMSO and a hydronium ion from $\mathbf{C_1}$ resulting in the endergonic formation of **D** (−2.1 kcal/mol) (**C** → **D**, +2.5 kcal/mol). The optimized structures of $\mathbf{C_1}$ and $\mathbf{C_2}$ are also shown in Fig. 10. Note that addition of water, as shown in Fig. 10 stabilizes the intermediate $\mathbf{C_1}$ (shown

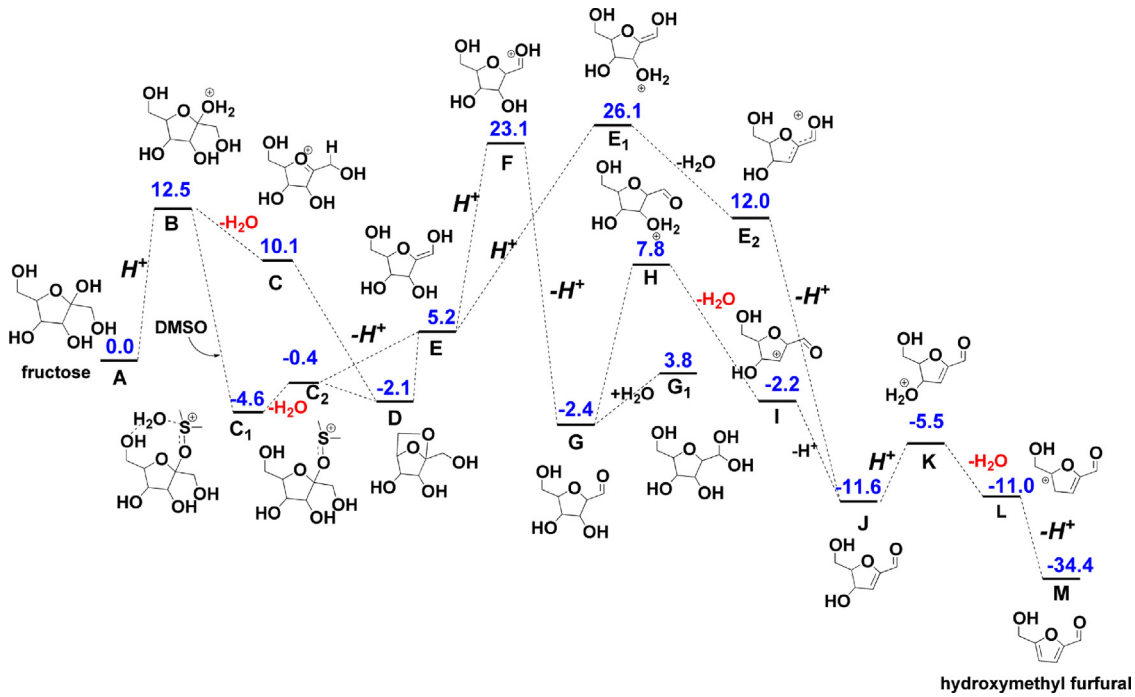

Fig. 9. Computed Gibbs free energy profile for the fructose-HMF reaction pathway. All energies (kcal/mol) are computed using the G4MP2 level of theory and w.r.t. the free energy of isolated fructose molecule in DMSO medium. The DMSO medium was included implicitly with a continuum model (see Section 2.7) except in some cases as noted where an explicit DMSO molecule is included. Optimized geometries of species C1 and C2 are shown in Fig. 9. Formation of E and D is upon the removal of protonated DMSO from C2 (see text).

as $\mathbf{C_1}$ + 1 water), by providing a hydrogen bonding network and strengthening the C—O_{DMSO} bond. This suggests the possibility of water exchange indicated by our ^{17}O labeling study. Species **D** is an identified intermediate during the fructose-HMF pathway in DMSO [36]. Alternatively, **D** can be formed via the pathway $\mathbf{C_1} \rightarrow \mathbf{C} \rightarrow \mathbf{D}$, where the $\mathbf{C_1} \rightarrow \mathbf{C}$ involves the detachment of DMSO and H_2O from C_1. In this pathway $\mathbf{C_1}$ to **C** is endergonic by 14.7 kcal/mol, while **C** to **D** is exergonic by 12.2 kcal/mol. Both species $\mathbf{C_2}$ and **D** can lead to the enol **E** (5.2 kcal/mol). Note that detailed kinetic information (both experimental and theoretical) regarding these intermediates are essential to understand the relative abundance of these various intermediates during the initial dehydration. Experimental data is being generated to allow us to formulate such a model but the kinetics involved in such a model are beyond the scope of the current work.

Int. 3 observed in this study and previous reported studies [33,34,40] is 4-(hydroxy)-5-(hydroxymethyl)-4,5-dihydrofuran-2-carbaldehyde, shown as species **J** in Fig. 9. The formation of **J** (−11.6 kcal/mol) from **E** (+5.2 kcal/mol), proposed here through pathway $\mathbf{E} \rightarrow \mathbf{E_1} \rightarrow \mathbf{E_2} \rightarrow \mathbf{J}$, involves protonation, dehydration and deprotonation respectively. Alternatively, **J** can be formed via a pathway $\mathbf{E} \rightarrow \mathbf{F} \rightarrow \mathbf{G} \rightarrow \mathbf{H} \rightarrow \mathbf{I} \rightarrow \mathbf{J}$, which involves acid catalyzed enol to ketone tautomerization and subsequent dehydration. Int. 2, determined experimentally may either be species **E** or species **G**. The relative free energy of **J** clearly indicates the stability of this intermediate with respect to fructose and supports the experimental observations relating to **Int. 3** discussed above. Similar to the formation of **J** from **E**, the formation of HMF (**M**, −34.4 kcal/mol) involves protonation, dehydration, and deprotonation via the $\mathbf{J} \rightarrow \mathbf{K} \rightarrow \mathbf{L} \rightarrow \mathbf{M}$ pathway. Species **K** and **L** have

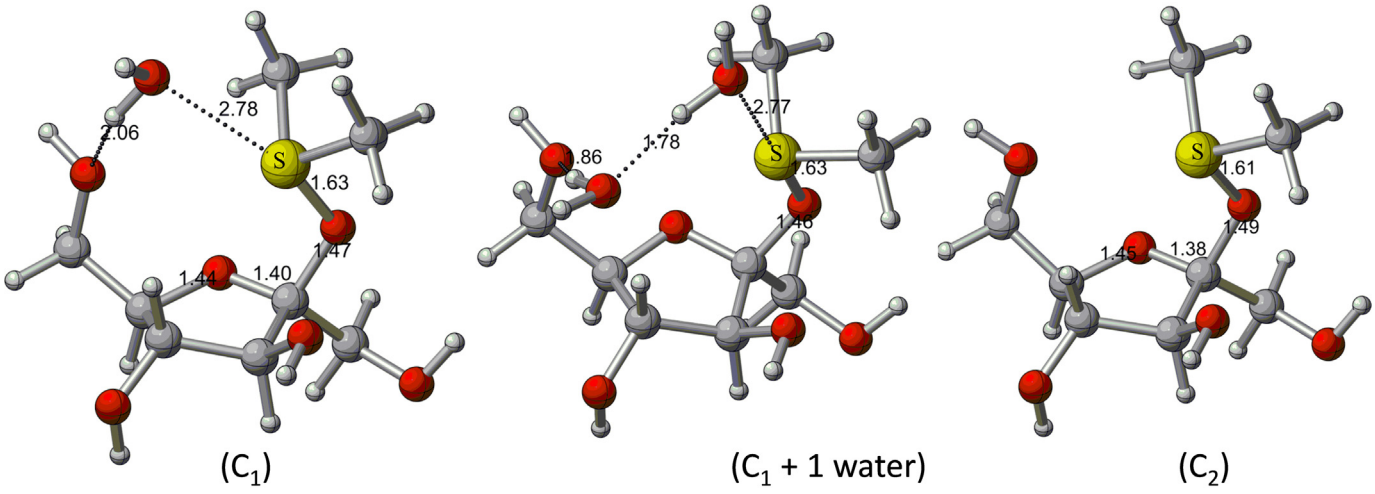

Fig. 10. Optimized structures of intermediates (C1, C1 + 1 water, and C2) at the B3LYP/6-31G(2df,p) level of theory used for geometries in G4MP2 theory.

relative free energies similar to that of fructose, however the formation of HMF is significantly exergonic (by 30 kcal/mol) suggesting that thermodynamic equilibrium would favor the formation of HMF, indicating the experimental observation of **K** and **L** species, which have not been observed, is less likely.

The free energy landscape presented in Fig. 9 clearly supports the experimentally identified intermediates: **Int. 1**, **Int. 2**, and **Int. 3** (species $\mathbf{C_1}$, **E** or **G**, and **J**, respectively). Though the calculation of the free energy of the intermediates indicates that the keto form of **Int.2** (**G**) is lower in energy than its enol counterpart (**E**), the steady state concentration of the intermediates which is relevant for experimental detection is determined by the kinetics of formation and reaction of a given species. Calculation of the relevant kinetic parameters is beyond the scope of the current computational study and thus theory does not allow us to reach an unambiguous conclusion as to whether species **E** or **G** is present a higher concentration under a given set of experimental conditions. Additionally, other low energy structures such as species **D** (anhydrofructose) and $\mathbf{G_1}$ (diol) were proposed elsewhere [34,40]. We also note that explicit inclusion of solvent molecules in the model would stabilize the positively charged species considerably. A detailed kinetic model including the explicit effects of solvent molecules in the formation of various intermediates in the fructose-HMF pathway is currently under investigation.

4. Conclusions

The mechanism of the acid catalyzed dehydration of D-fructose in DMSO was probed experimentally by means of ^{13}C, ^{1}H and ^{17}O NMR and high-resolution electrospray mass-spectroscopy, and theoretically using high level G4MP2 theory. Two intermediates, 2-(hydroxydimethylsulfinyloxy)-β-D-fructofuranose (**Int. 1**) and 4-(hydroxy)-5-(hydroxymethyl)-4,5-dihydrofuran-2-carbaldehyde (**Int. 3**) were unambiguously identified by both theory and experiment. A third species that is capable of keto–enol tautomerism (**Int. 2**) 2-(hydroxymethyl)-5-(hydroxylmethylene)-tetrahydrofuran-3,4-diol (enol form) and 4-dihydroxy-5-hydroxymethyl-tetrahydro-furan-2-carbaldehyde (the keto form) was also identified by theory and experimentally by MS; however experimentally it was not possible in this study to distinguish between the keto and the enol forms. The results of theoretical calculations indicate that both the enol and keto forms are local minima on the potential energy surface and the keto form has a lower free energy than the enol form. Our calculations and experimental results provide evidence for an intermediate (**Int. 1**) that has not been previously reported and demonstrate the role the solvent plays in the reaction mechanism. We also report preliminary kinetic data, using NMR spectroscopy that is consistent with the proposed intermediates. Three dehydration steps are required to go from fructose to HMF. Since such reactions are typically acid catalyzed, it is not surprising that the experimentally observed intermediates are the same for the two Brønsted acid catalysts that we have used. We also observe the same intermediates along the reaction pathway to HMF when using PO_4^{3-}/niobic acid, which has both Lewis acid and Brønsted acid sites. These results are consistent with there being a common mechanism for the acid catalyzed triple dehydration of fructose to produce HMF and, at least for the systems studied; this mechanism appears to be independent of the source of protons. We also note that, in presence of oxygen, DMSO can decompose at moderate temperatures to produce acidic species that catalyze the dehydration of fructose, thus rationalizing the claim in the literature that DMSO can act as a catalyst for the fructose dehydration reaction.

Acknowledgements

The authors thank Dr. Yuyang Wu and Jaekuk Kim of Northwestern University for NMR and LC–MS technical assistance. We also acknowledge Prof. Karl Scheidt for his valuable discussions with regard to the possibility of complexation of DMSO with the dehydrated fructose species that form **Int. 1**. We thank Dr. Weiqiang Wu for his help in characterizing acid sites on PO_4^{3-}/niobic acid. This work has been supported as part of the Institute for Atom-efficient Chemical Transformations (IACT), an Energy Frontier Research Center funded by the U.S. Department of Energy, Office of Science, Office of Basic Energy Sciences. We gratefully acknowledge grants of computer time from EMSL, a national scientific user facility located at Pacific Northwest National Laboratory, the ANL Laboratory Computing Resource Center (LCRC), and the ANL Center for Nanoscale Materials. This research used resources of the National Energy Research Scientific Computing Center, which is supported by the Office of Sciences of the U.S. Department of Energy under Contract no. DE-AC02-05CH11231

Appendix A. Supplementary data

Supplementary data associated with this article can be found, in the online version, at http://dx.doi.org/10.1016/j.apcatb.2014.10.056.

References

[1] F.W. Lichtenthaler, Acc. Chem. Res. 35 (2002) 728–737.
[2] A. Corma, S. Iborra, A. Velty, Chem. Rev. 107 (2007) 2411–2502 (Washington, DC, U. S.).
[3] J.N. Chheda, G.W. Huber, J.A. Dumesic, Angew. Chem., Int. Ed. 46 (2007) 7164–7183.
[4] A.A. Rosatella, S.P. Simeonov, R.F.M. Frade, C.A.M. Afonso, Green Chem. 13 (2011) 754–793.
[5] Q. Bao, K. Qiao, D. Tomida, C. Yokoyama, Catal. Commun. 9 (2008) 1383–1388.
[6] V.V. Ordomsky, d.S.J. van, J.C. Schouten, T.A. Nijhuis, J. Catal. 287 (2012) 68–75.
[7] C.O. Tuck, E. Perez, I.T. Horvath, R.A. Sheldon, M. Poliakoff, Science 337 (2012) 695–699 (Washington, DC, U. S.).
[8] Y. Qu, C. Huang, J. Zhang, B. Chen, Bioresour. Technol. 106 (2012) 170–172.
[9] A.H. Jadhav, H. Kim, I.T. Hwang, Catal. Commun. 21 (2012) 96–103.
[10] M. Marzo, A. Gervasini, P. Carniti, Catal. Today 192 (2012) 89–95.
[11] C.P. Locas, V.A. Yaylayan, J. Agric. Food Chem. 56 (2008) 6717–6723.
[12] K. Hamada, H. Yoshihara, G. Suzukamo, Chem. Lett. (1982) 617–618.
[13] F.S. Asghari, H. Yoshida, Ind. Eng. Chem. Res. 45 (2006) 2163–2173.
[14] Y. Roman-Leshkov, C.J. Barrett, Z.Y. Liu, J.A. Dumesic, Nature (London, UK) 447 (2007) 982–985.
[15] H. Zhao, J.E. Holladay, H. Brown, Z.C. Zhang, Science 316 (2007) 1597–1600.
[16] K.-I. Seri, Y. Inoue, H. Ishida, Chem. Lett. (2000) 22–23.
[17] H. Ishida, K.-i. Seri, J. Mol. Catal. A: Chem. 112 (1996) L163–L165.
[18] P. Rivalier, J. Duhamet, C. Moreau, R. Durand, Catal. Today 24 (1995) 165–171.
[19] M.A. Schwegler, P. Vinke, d.E.M. Van, B.H. Van, Appl. Catal., A: Gen. 80 (1992) 41–57.
[20] Y. Roman-Leshkov, J.N. Chheda, J.A. Dumesic, Science 312 (2006) 1933–1937.
[21] C. Lansalot-Matras, C. Moreau, Catal. Commun. 4 (2003) 517–520.
[22] T. Armaroli, G. Busca, C. Carlini, M. Giuttari, G.A.M. Raspolli, G. Sbrana, J. Mol. Catal. A: Chem. 151 (2000) 233–243.
[23] C. Carlini, M. Giuttari, G.A.M. Raspolli, G. Sbrana, T. Armaroli, G. Busca, Appl. Catal., A: Gen. 183 (1999) 295–302.
[24] C. Carlini, P. Patrono, G.A.M. Raspolli, G. Sbrana, Appl. Catal., A: Gen. 275 (2004) 111–118.
[25] F. Benvenuti, C. Carlini, P. Patrono, G.A.M. Raspolli, G. Sbrana, M.A. Massucci, P. Galli, Appl. Catal., A: Gen. 193 (2000) 147–153.
[26] K.-I. Seri, Y. Inoue, H. Ishida, Bull. Chem. Soc. Jpn. 74 (2001) 1145–1150.
[27] M. Watanabe, Y. Aizawa, T. Iida, T.M. Aida, C. Levy, K. Sue, H. Inomata, Carbohydr. Res. 340 (2005) 1925–1930.
[28] M. Watanabe, Y. Aizawa, T. Iida, R. Nishimura, H. Inomata, Appl. Catal., A: Gen. 295 (2005) 150–156.
[29] C. Moreau, R. Durand, S. Razigade, J. Duhamet, P. Faugeras, P. Rivalier, P. Ros, G. Avignon, Appl. Catal., A: Gen. 145 (1996) 211–224.
[30] F.S. Asghari, H. Yoshida, Ind. Eng. Chem. Res. 46 (2007) 7703–7710.
[31] S.K. Tyrlik, D. Szerszen, M. Olejnik, W. Danikiewicz, Carbohydr. Res. 315 (1999) 268–272.
[32] L. Cottier, G. Descotes, Trends Heterocycl. Chem. 2 (1991) 233–248.

[33] A.S. Amarasekara, L.D. Williams, C.C. Ebede, Carbohydr. Res. 343 (2008) 3021–3024.
[34] H. Kimura, M. Nakahara, N. Matubayasi, J. Phys. Chem. A 117 (2013) 2102–2113.
[35] T.M. Santosusso, D. Swern, J. Org. Chem. 41 (1976) 2762–2768.
[36] W.N. Haworth, W.G.M. Jones, J. Chem. Soc. (1944) 667–670.
[37] H.E. van Dam, A.P.G. Kieboom, B.H. Van, Starch 38 (1986) 95–101.
[38] B.F.M. Kuster, Starch 42 (1990) 314–321.
[39] M.J. Antal Jr., W.S.L. Mok, G.N. Richards, Carbohydr. Res. 199 (1990) 91–109.
[40] G.R. Akien, L. Qi, I.T. Horvath, Chem. Commun. (Cambridge, UK) 48 (2012) 5850–5852.
[41] J. Zhang, E. Weitz, ACS Catal. 2 (2012) 1211–1218.
[42] M. Tamura, K.-i. Shimizu, A. Satsuma, Appl. Catal., A: Gen. 433–434 (2012) 135–145.
[43] L.A. Curtiss, P.C. Redfern, K. Raghavachari, J. Chem. Phys. 127 (2007), 124105/124101–124105/124105.
[44] R.S. Assary, P.C. Redfern, J.R. Hammond, J. Greeley, L.A. Curtiss, J. Phys. Chem. B 114 (2010) 9002–9009.
[45] R.S. Assary, P.C. Redfern, J. Greeley, L.A. Curtiss, J. Phys. Chem. B 115 (2011) 4341–4349.
[46] R.S. Assary, L.A. Curtiss, Energy Fuels 26 (2012) 1344–1352.
[47] A.V. Marenich, C.J. Cramer, D.G. Truhlar, J. Phys. Chem. B 113 (2009) 6378–6396.
[48] M.J. Frisch, Gaussian Inc., Wallingford, CT, 2009.
[49] D.J. Nicole, B. Gillet, E.N. Eppiger, J.J. Delpuech, Tetrahedron Lett. 23 (1982) 1669–1672.
[50] M. Jaseja, A.S. Perlin, P. Dais, Magn. Reson. Chem. 28 (1990) 283–289.
[51] F. Jiang, Q. Zhu, D. Ma, X. Liu, X. Han, J. Mol. Catal. A: Chem. 334 (2011) 8–12.
[52] B.F.M. Kuster, L.M. Tebbens, Carbohydr. Res. 54 (1977) 159–164.
[53] L.B. Krivdin, G.A. Kalabin, Prog. Nucl. Magn. Reson. Spectrosc. 21 (1989) 293–448.
[54] B. Bose, S. Zhao, R. Stenutz, F. Cloran, P.B. Bondo, G. Bondo, B. Hertz, I. Carmichael, A.S. Serianni, J. Am. Chem. Soc. 120 (1998) 11158–11173.
[55] X. Creary, E.A. Burtch, Z. Jiang, J. Org. Chem. 68 (2003) 1117–1127.
[56] M.G.M. Gonzalez, R.S. Assary, J. Dumesic, L.A. Curtiss, Energy Environ. Sci. 5 (2012) 6981–6989.